A charge-driven molecular water pump

XIAOJING GONG[1,2], JINGYUAN LI[3], HANGJUN LU[1,2,4], RONGZHENG WAN[1], JICHEN LI[5], JUN HU[1,6]* AND HAIPING FANG[1]*

[1]Shanghai Institute of Applied Physics, Chinese Academy of Sciences, PO Box 800-204, Shanghai 201800, China
[2]Graduate School of the Chinese Academy of Sciences, Beijing 100080, China
[3]Department of Physics, Zhejiang University, Hangzhou, 310027, China
[4]Department of Physics, Zhejiang Normal University, 321004, Jinhua, China
[5]Department of Physics and Astronomy, The University of Manchester, Manchester M60 1QD, UK
[6]Bio-X Life Sciences Research Center, College of Life Science and Technology, Shanghai JiaoTong University, Shanghai 200030, China
*e-mail: jhu@sjtu.edu.cn; fanghaiping@sinap.ac.cn

Published online: 21 October 2007; doi:10.1038/nnano.2007.320

Understanding and controlling the transport of water across nanochannels is of great importance for designing novel molecular devices, machines and sensors and has wide applications[1–9], including the desalination of seawater[5]. Nanopumps driven by electric or magnetic fields can transport ions[10,11] and magnetic quanta[12], but water is charge-neutral and has no magnetic moment. On the basis of molecular dynamics simulations, we propose a design for a molecular water pump. The design uses a combination of charges positioned adjacent to a nanopore and is inspired by the structure of channels in the cellular membrane that conduct water in and out of the cell (aquaporins). The remarkable pumping ability is attributed to the charge dipole-induced ordering of water confined in the nanochannels[13,14], where water can be easily driven by external fields in a concerted fashion. These findings may provide possibilities for developing water transport devices that function without osmotic pressure or a hydrostatic pressure gradient.

Conventional wisdom suggests that transporting water directionally through a nanochannel requires an osmotic or hydrostatic pressure gradient[5,15]. Such a method would involve a large reservoir of solution on one side of the channel to produce the pressure gradient. Macroscopically, mechanical pumps are widely used to transport water. However, at the nanometre level, the active transportation of water through nanochannels (water nanopumps) is technically difficult or even impossible using mechanisms comparable to those used macroscopically. Progress in moving water has been made by designing systems with an imbalance of surface tension[16] or a chemical[17] or thermal gradient[18], but it is still difficult to make a controllable continuous unidirectional water flow.

Water molecules confined in nanoscale channels usually exhibit dynamics different from bulk systems[13–15,19–24]. Rather than enhancing water flow by a ring of charges[24] and gating of the water permeation by a single charge[14] positioned near a nanochannel, here, a biased potential is produced by the assignment of three charges with asymmetric positions adjacent to the pore, and the potential barrier in the system remains small enough to allow water permeation across the channel.

We used the uncapped armchair single-walled carbon nanotube (SWNT) as the model system. Carbon nanotubes have outstanding potentials for applications in nanoscale sensors, devices and machines[2,4,6–12,23]. The molecular configuration in our arrangement consisted of an SWNT 23 Å in length and 8.1 Å in diameter, embedded along the vertical direction between two graphite sheets (Fig. 1). Three positive charges with charge magnitudes of 1.0*e*, 0.5*e* and 0.5*e* are positioned at $z = -d$, -0.7 Å and 0.7 Å, respectively, where $z = 0$ corresponds to the centre of the channel and the position of the largest charge, *d*, is a variable in our simulations. All of the positive charges are at the same radial distance δ from the carbon atoms, where δ is also a variable in our model. To keep the whole system electrically neutral, negative charges are assigned close to the left boundary of the carbon sheet with the same *z*-values as the positive charges. It was numerically determined that the existence of the negative charges does not change the results obtained from this study. For the purpose of discussion, we refer to this particular charge configuration as the ‘main’ system.

The idea to use this structure of charges is inspired by the charge distribution of conserved regions in biological channels called aquaporins. (See Supplementary Information for a discussion of the experimental possibility of designing water molecular pumps according to this architecture.) We used molecular dynamics to simulate the SWNT and graphite sheets solvated in a water reservoir for 120 ns for different charge arrangements of values δ and *d*. The last 115 ns were collected for analysis. We define the flow as the total number of water molecules per nanosecond that leave the SWNT from one end, having entered the opposite side. Similarly, the net flux is the difference between the number of water molecules per nanosecond leaving from one end and the other (again having entered from the opposite end). To our surprise, 337 water molecules passed from top to bottom in the channel, and only three water molecules penetrated along the opposite direction, resulting in a net flux of over 2.8 water molecules per nanosecond crossing the channel when $\delta = 0.5$ Å and $d = 7.9$ Å. This average net flux is one order of magnitude larger than the experimentally observed flux through an SWNT with diameter of less than two nanometres, under an external pressure gradient of 1 atm (ref. 6), and is also comparable to the measured rate of 3.0 per nanosecond per channel for aquaporin-1 (a kind of aquaporin) at a low osmotic pressure[25]. The nanochannel therefore functions as an excellent controllable molecular pump.

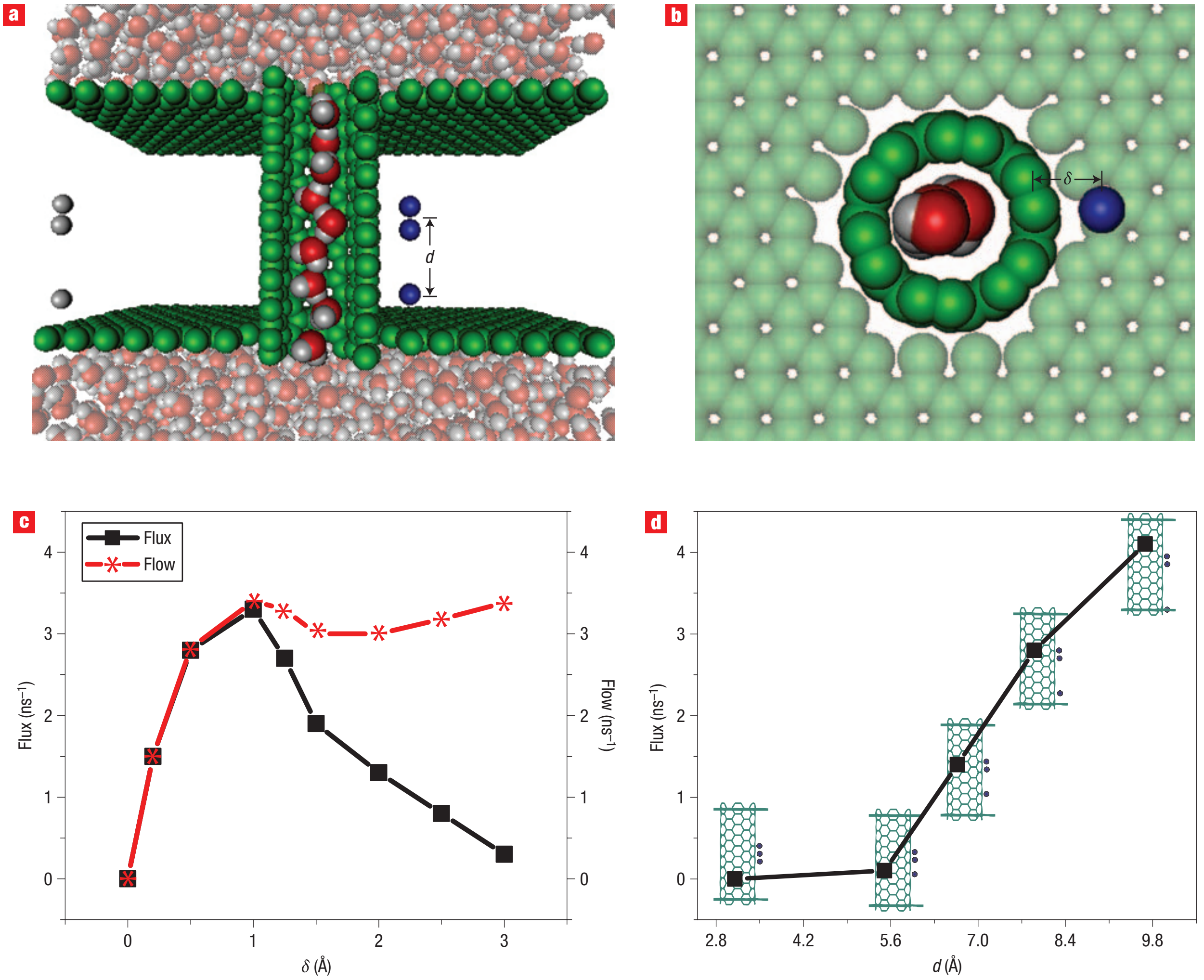

Figure 1 Introduction to the main system and the flows and fluxes for different charge arrangements in the main system. a, Side view of the main system. The green spheres are the carbon atoms of the nanotube and the graphite sheets (note that the figure is not drawn to scale). The blue points are the positive charges (0.5*e*, 0.5*e* and 1.0*e*, from top to bottom), and the grey ones are negative charges to neutralize the positive charges near the channel. Water molecules are shown in sphere representation with oxygen in red and hydrogen in grey. **b**, Top view of the same arrangement. **c**, Flow and flux for different radial distance δ for $d = 7.9$ Å. **d**, Flux with respect to *d* for $\delta = 0.5$ Å.

Table 1 Electrostatic potential barriers of water–charge interactions (ΔE), together with the flows and fluxes for the different systems.

System type	ΔE (kJ mol^{-1})	Flow (ns^{-1})	Flux (ns^{-1})
Main system	40.5	2.8	2.8
Bottom system	58.7	0.1	0.1
Middle system	45.3	0.1	0
Merged system	49.5	0.8	0.4

A series of simulations with different charge arrangements were studied to maximize the flux. We found that the net flux and flow are very sensitive to δ, as shown in Fig. 1c. There is an obvious net flux for $0.2 < \delta < 2.5$ Å with a peak at $\delta \approx 1.0$ Å. When δ approaches zero, both the average flow and flux become negligible, showing that the nanochannel is closed[14,15]. When δ is greater than 1 Å, the flow maintains the same level of ~3 ns^{-1}; however, the flux is reduced because of the decreasing asymmetrical interaction between the charges and the water inside the SWNT. Eventually, the channel's behaviour becomes similar to the charge-free systems. A separate study of how flux depends on the distance *d* is illustrated in Fig. 1d. The simulation shows that the larger the value of *d*, the larger the flux. When *d* is less than 5.6 Å, about the width of two water molecules, the flux could not be initiated.

To understand how the particular charge configuration affects the water dynamics in the channel, we compared the behaviour of the main system with systems having only some of the charges. These systems with charge(s) only in the bottom or middle position are referred to as the 'bottom' and 'middle' systems, respectively. The positions of those charges relative to the nanotube are the same as those in the main system, with $\delta = 0.5$ Å. The flows in both systems are very small, on the order of 0.1 ns^{-1}, consistent with our previous observations[14]. The middle system is symmetrical and has no net flux. The asymmetrical structure of the bottom system makes the water permeation across the channel asymmetrical in the main system (see Table 1). However, the simulation results show that the flux can only be initiated in the main system.

Figure 2a shows the electrostatic potential of the water molecules with the charge(s) versus vertical position along the SWNT. ‘Valleys’ are obvious in regions closest to the charges. The valley for the bottom system is much deeper than the corresponding valley for the main system. The potential barrier, which is defined as the difference between the maximum and minimum of the potential profile, is usually used to characterize the potential profile. As displayed in Table 1, the potential barrier of the bottom system is much larger than that of the main system. Consequently, it is reasonable that water permeates the main system more easily than the bottom system.

The potential barrier for the middle system is slightly larger than that for the main system, so the potential barrier cannot explain the large difference between the flow values for these two systems. We note that the electrical field is symmetrical in the middle system and asymmetrical in the main system. Remarkably, if we apply an artificial osmotic pressure difference[15] of about 560 MPa between the two ends of the nanochannel in the middle system, we can obtain a net flux (≈flow) of 2.8 ns^{-1}, comparable with the flux in the main system; that is, water permeation for the middle system with the additional appropriate pressure gradient is quite similar to the water permeation of the main system. The result clearly shows that the barriers for both the middle system and the main system are high enough to exclude water permeation caused by thermal fluctuations, whereas in the main system an asymmetrical potential between two ends of the tube can result in a unidirectional flow. Consequently, the bottom charge in the main system provides a large asymmetrical electric potential, whereas the two charges in the middle of the system greatly lower the potential barriers.

The distribution of the average water dipole orientation angle $\langle\theta\rangle$ along the length of the channel is shown in Fig. 2b. For all systems, $\langle\theta\rangle$ lies between $\sim 150^\circ$ and $\sim 30^\circ$. The water dipoles near the bottom end point down, whereas the water dipoles near the top end point up, showing a bipolar order. In the bottom and middle systems, an abrupt change in the distribution of $\langle\theta\rangle$ happens in the position facing the charge(s). Correspondingly, there is a large potential well coinciding with the positions of the bottom/middle charge(s). $\langle\theta\rangle$ oscillates several times in the main system between the positions of the bottom charge and the middle charges, corresponding to a transient of $\langle\theta\rangle$ changing from $\sim 150^\circ$ to $\sim 30^\circ$. Meanwhile, for the main system, the potential wells at the charge positions are less deep. It is clear that the longer the length for the transient, the less the depths of the potential wells, and hence the easier the water permeation across the channel. This is consistent with the simulation results shown in Fig. 1d; that is, the larger the value of d, the larger flux. We note that the single-file structure of water inside the channel is crucial to the water dipole orientation distribution being shielded from thermal fluctuations; for wider channels, the abrupt changes in the distribution of $\langle\theta\rangle$ at the positions facing the charges will be reduced by thermal fluctuations, which smoothes the asymmetries of the potentials and weakens the pumping abilities. It should be emphasized that an interior bipolar water orientation, believed to prevent proton transport, together with a less deep potential well to make water permeation easy, provided by the distribution of charges in the main system, is just what researchers expected for aquaporins (refs 14, 26).

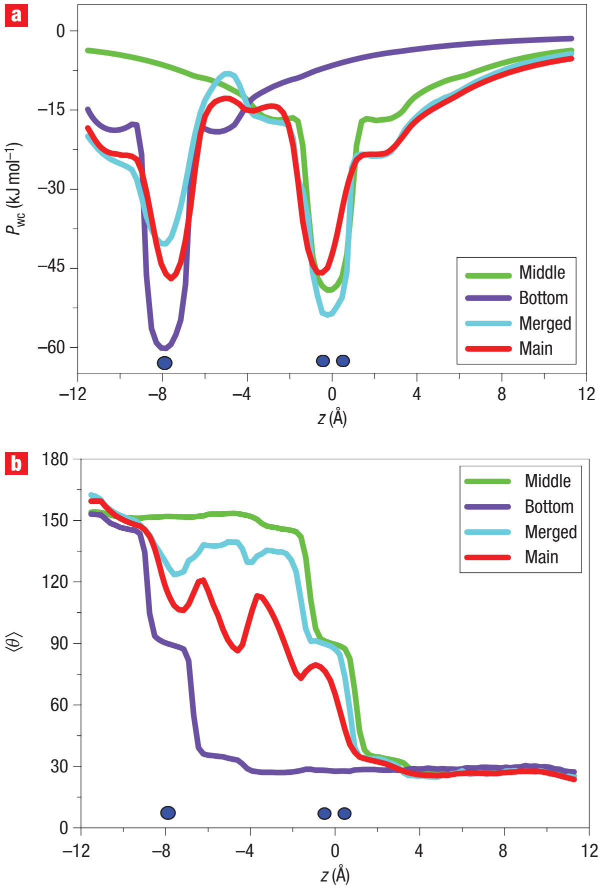

Figure 2 Water–charge interaction and the averaged dipole orientation of water molecules inside the SWNT. a, Interaction energies, P_{WC}, of a water molecule at z with the charge(s) for the main system (red), bottom system (purple), middle system (green) and merged system (cyan), respectively. **b**, Profile of $\langle\theta\rangle$ along the channel, where θ is the angle between a water dipole and the nanotube axis (z-axis), and the average is taken over all the data from simulations. The blue filled circles denote the locations of the charges. It can be seen that each of the valleys of the electrostatic potential corresponds to a transition of $\langle\theta\rangle$.

The method of using two $+0.5e$ charges positioned in the middle of the channel is very important. If we merged them into one $+1.0e$ charge at $z = 0$ (this system is called a ‘merged system’) the permeation behaviour would be qualitatively different. In Fig. 2 and Table 1, we illustrate that the barrier increases considerably, and the net flux is reduced to only 0.4 ns^{-1}, significantly smaller than the flux for the main system. We also note that the remarkable pump ability remains when the distance between the two middle charges increases to a certain extent, and a unidirectional flux of 4.4 ns^{-1} was observed when this distance doubled.

One may argue that the pump we designed looks like a perpetual mobile. We should point out that extra energy is required to constrain the charges at their original positions, which is the key to the pumping ability. We found that the electrostatic forces exerted by water molecules on the three charges are 533 pN, 313 pN and 300 pN, from the lower to upper charges, respectively, as averaged from all the simulations. Without the constraint, the charges would be forced away and the net flux would vanish (see Supplementary Information for details).

Finally, we note that the pumping ability described here can be directly applied to insulator nanochannels, which may be fabricated in the near future. It can also be extended to semiconductor nanopores, such as armchair SWNTs with finite length or zigzag SWNTs. In these systems, it will be necessary to account for the effects of screening, and the charges we used here should be regarded as effective charges—the realistic charges should be made larger by multiplication of a factor related to the screening effect. The positions of the charges may be left unchanged.

METHODS

MOLECULAR DYNAMICS SIMULATIONS

All simulations were carried out at a constant pressure of 1 bar, a temperature of 300 K and an initial box size $L_x = 5.0$ nm, $L_y = 5.0$ nm and $L_z = 6.0$ nm with Gromacs 3.3 (ref. 27) and by using the particle mesh Ewald method[28] for full electrostatics with a cutoff of 1 nm. Here the TIP3P water model[29] was applied. A time step of 2 fs was used, and data were collected every 1 ps. In the simulations, the carbon atoms were modelled as uncharged Lennard–Jones particles with a cross-section of $\sigma_{CC} = 0.34$ nm, $\sigma_{CO} = 0.3275$ nm, and a depth of the potential well of $\varepsilon_{CC} = 0.3612$ kJ mol^{-1}, $\varepsilon_{CO} = 0.4802$ kJ mol^{-1} (ref. 13). We found that this pumping ability is robust and that choosing a different water–carbon interaction potential[30] did not alter the conclusions. A carbon bond length of 0.14 nm and bond angle of 120° were maintained by harmonic potentials with spring constants of 393,960 kJ mol^{-1} and 527 kJ mol^{-1} rad^{-2} before relaxation[13]. In addition, a weak dihedral angle potential was applied to bonded carbon atoms[13]. We constrained the positions of the external charges and the carbon atoms at the inlet and outlet by using the position restraint. The two carbon sheets were held fixed. During the numerical simulations, we used position restraint to maintain the charged atoms at their original sites.

Received 13 April 2007; accepted 31 August 2007; published 21 October 2007.

References

1. Whitesides, G. M. The origins and the future of microfluidics. *Nature* **442**, 368–373 (2006).
2. Whitby, M. & Quirk, N. Fluid flow in carbon nanotubes and nanopipes. *Nature Nanotech.* **2,** 87–94 (2007).
3. Squires, T. M. & Quake, S. R. Microfluidics: fluid physics at the nanoliter scale. *Rev. Mod. Phys.* **77,** 977–1026 (2005).
4. Regan, B. C., Aloni. S., Ritchie, R. O., Dahmen, U. & Zettl, A. Carbon nanotubes as nanoscale mass conveyors. *Nature* **428,** 924–927 (2004).
5. Service, R. F. Desalination freshens up. *Science* **313,** 1088–1090 (2006).
6. Holt, J. K. *et al.* Fast mass transport through sub-2-nanometer carbon nanotubes. *Science* **312,** 1034–1037 (2006).
7. Bourlon, B., Wong, J., Miko, C., Forro, L. & Bockrath, M. A nanoscale probe for fluidic and ionic transport. *Nature Nanotech.* **2,** 104–107 (2007).
8. Besteman, K., Lee, J. O., Wiertz, F. G. M., Heering, H. A. & Dekker, C. Enzyme-coated carbon nanotubes as single-molecule biosensors. *Nano Lett.* **3,** 727–730 (2003).
9. Ghosh, S., Sood, A. K. & Kumar, N. Carbon nanotube flow sensors. *Science* **299,** 1042–1044 (2003).
10. Fan, R., Yue, M., Karnik, R., Majumdar, A. & Yang, P. D. Polarity switching and transient responses in single nanotube nanofluidic transistors. *Phys. Rev. Lett.* **95,** 086607 (2005).
11. Siwy, Z. & Fulinski, A. Fabrication of a synthetic nanopore ion pump. *Phys. Rev. Lett.* **89,** 198103 (2002).
12. Cole, D. *et al.* Ratchet without spatial asymmetry for controlling the motion of magnetic flux quanta using time-asymmetric drives. *Nature Mater.* **5,** 305–311 (2006).
13. Hummer, G., Rasaiah, J. C. & Noworyta, J. P. Water conduction through the hydrophobic channel of a carbon nanotube. *Nature* **414,** 188–190 (2001).
14. Li, J. Y. *et al.* Electrostatic gating of a nanometer water channel. *Proc. Natl Acad. Sci. USA* **104,** 3687–3692 (2007).
15. Zhu, F. Q. & Schulten, K. Water and proton conduction through carbon nanotubes as models for biological channels. *Biophys. J.* **85,** 236–244 (2003).
16. de Gennes, P. G., Brochard-Wyart, F. & Quere, D. Capillarity and Wetting Phenomena (Springer, New York, 2003).
17. Chaudhury, M. K. & Whitesides, G. M. How to make water run uphill. *Science* **256,** 1539–1541 (1992).
18. Linke, H. *et al.* Self-propelled Leidenfrost droplets. *Phys. Rev. Lett.* **96,** 154502 (2006).
19. Beckstein, O. & Sansom, M. S. P. Liquid–vapor oscillations of water in hydrophobic nanopores. *Proc. Natl Acad. Sci. USA* **100,** 7063–7068 (2003).
20. Majumder, M., Chopra, N., Andrews, R. & Hinds, B. J. Enhanced flow in carbon nanotubes. *Nature* **438,** 44 (2005).
21. Reiter, G. *et al.* Anomalous behavior of proton zero point motion in water confined in carbon nanotubes. *Phys. Rev. Lett.* **9724,** 7801 (2006).
22. Sun, L. & Crooks, R. Single carbon nanotube membranes: a well-defined model for studying mass transport through nanoporous materials. *J. Am. Chem. Soc.* **122,** 12340–12345 (2000).
23. Tenne, R. Inorganic nanotubes and fullerene-like nanoparticles. *Nat. Nanotechnol.* **1,** 103–111 (2006).
24. Joseph, S., Mashl, R. J., Jakobsson, E. & Arulu, N. R. Electrolytic transport in modified carbon nanotubes. *Nano Lett.* **3,** 1399–1403 (2003).
25. Zeidel, M. L. *et al.* Ultrastructure, pharmacologic inhibition, and transport selectivity of aquaporin channel-forming integral protein in proteoliposomest. *Biochemistry* **33,** 1606–1615 (1992).
26. de Groot, B. L. & Grubmüller, H. Water permeation across biological membranes: mechanism and dynamics of aquaporin-1 and GlpF. *Science* **294,** 2353–2357 (2001).
27. Hess, B. *et al.* *Gromacs-3.3* (Department of Biophysical Chemistry, University of Groningen, 2005).
28. Darden, T. A., York, D. M. & Pedersen, L. G. Particle mesh Ewald: An *N*·log(*N*) method for Ewald sums in large systems. *J. Chem. Phys.* **98,** 10089–10092 (1993).
29. Jorgensen, W. L., Chandrasekhar, J., Madura, J. D., Impey, R. W. & Klein, M. L. Comparison of simple potential functions for simulating liquid water. *J. Chem. Phys.* **79,** 926–935 (1983).
30. Longhurst, M. J. & Quirke, N. The environmental effect on the radial breathing mode of carbon nanotubes in water. *J. Chem. Phys.* **124,** 234708 (2006).

Acknowledgements

We thank P. A. Pincus, D. Bensimon, Ruhong Zhou, Chunhai Fan and Jun Yan for helpful discussions. This work was supported by grants from Chinese Academy of Sciences, the National Science Foundation of China under grants nos. 10474109 and 10674146, the National Basic Research Program of China under grant nos. 2007CB936000, 2006CB933000 and 2006CB708612, and Shanghai Supercomputer Center of China.
Correspondence and requests for materials should be addressed to H.P.F. and J.H.
Supplementary information accompanies this paper on www.nature.com/naturenanotechnology.

Author contributions

X.J.G. performed most of the numerical simulations. H.P.F. and X.J.G. carried out most of the theoretical analysis. J.Y.L., H.J.L. and R.Z.W. carried out some numerical simulations and theoretical analysis. H.P.F., J.H., X.J.G. and J.C.L. contributed most of the ideas and wrote the paper. All authors discussed the results and commented on the manuscript.

Reprints and permission information is available online at http://npg.nature.com/reprintsandpermissions/

Copyright of Nature Nanotechnology is the property of Nature Publishing Group and its content may not be copied or emailed to multiple sites or posted to a listserv without the copyright holder's express written permission. However, users may print, download, or email articles for individual use.